mulation and also predicts the surface location of Pla. The plasminogen activation and chemoattractant reduction hypotheses are not mutually exclusive. These two mechanisms may be synergistic by affecting both cellular and noncellular processes contributing to containment of the bacteria. Direct in vivo tests of hypotheses regarding Pla activity will be essential to understand its mechanism of action.

Whatever the mechanism of Pla action, our findings may have broad implications for other Gram-negative infections. Homologs of *pla* have been found in *Escherichia coli* (*ompT*, 50% homology) and *Salmonella typhimurium* (*prtA*, 70% homology) (*14*). We have recently sequenced another in *Salmonella typhi* that is very similar to the *S. typhimurium* gene. In all of these organisms, the *pla* homologs are chromosomal and have no known physiological function. The role of Pla in plague implies that this class of proteases may contribute, in a more subtle way, to the capacity of less virulent species to produce disseminated infection. Such infections are a major source of mortality for immunocompromised patients. As we have noted (*14*), the homologies described above also suggest that *Y. pestis* acquired *pla* from a member of the *Salmonella* lineage. Given the importance of this gene to the life cycle of *Y. pestis* in nature, acquisition of the pPCP1 plasmid was clearly a major event in the evolution of this pathogen from *Y. pseudotuberculosis*. This argues against the notion that *Y. pestis* has arisen repeatedly from *Y. pseudotuberculosis* by acquisition of gene-inactivating mutations (*18*). It also presents another example of the importance of mobile genetic elements in the evolution of bacterial virulence.

REFERENCES AND NOTES

1. H. Bercouvier and H. H. Mollaret, in *Bergeys Manual of Systematic Bacteriology*, N. R. Kreig and J. G. Holt, Eds. (Williams and Wilkins, Baltimore, 1984), vol. 1, pp. 498–509.
2. R. R. Brubaker, E. D. Beesley, M. J. Surgalla, *Science* **149**, 422 (1965).
3. T. Butler, *Plague and Other* Yersinia *Infections* (Plenum, New York, 1983), pp. 118–140.
4. O. A. Sodeinde and J. D. Goguen, *Infect. Immun.* **56**, 2743 (1988).
5. E. D. Beesley, R. R. Brubaker, W. A. Jansen, M. J. Surgalla, *J. Bacteriol.* **165**, 19 (1967).
6. M. J. Finegold, J. J. Petery, R. F. Berendt, H. V. Adams, *Am. J. Pathol.* **53**, 99 (1961).
7. Human Glu-plasminogen (10 μM) was incubated with purified Pla-containing *E. coli* outer membranes (~2 μM Pla) in 0.1 M tris-HCl buffer (pH 7.5) for 20 min at 37°C. Bacterial membranes were removed by centrifugation, and a sample of the supernatant was separated on an SDS-polyacrylamide gel. A sample of the same plasminogen activated with urokinase was run in an adjacent lane for comparison and was indistinguishable from the Pla-treated sample. A larger amount of the supernatant was separated on a preparative gel and transferred to Immobilon-P (Millipore). The band corresponding to the light chain of urokinase-activated plasmin was excised and the NH_2-terminal sequence determined.
8. J. H. Verheijen, E. Mullart, G. T. G. Chang, G. Wijngaards, *Thromb. Haemostasis* **48**, 266 (1982).
9. R. Lottenberg, U. Christensen, C. M. Jackson, P. L. Coleman, *Methods Enzymol.* **80**, 341 (1981).
10. S. W. Peltz, T. A. Hardt, W. F. Mangel, *Biochemistry* **21**, 2798 (1982).
11. M. Hoylaerts, D. C. Rijken, H. R. Lijnen, D. Collen, *J. Biol. Chem.* **257**, 2912 (1982).
12. Seventy-five microliters of fresh human or rat plasma were added to 150 μl of 0.1 M phosphate buffer (pH 7.2) containing 2 units of human thrombin and a range of concentrations of either Pla [as purified outer membranes from the *E. coli* Pla over-producer BL21(DE3, pPLA100)] or human urokinase. Clots formed immediately, and the time required for complete lysis was observed. The logarithm of lysis time was plotted against the logarithm of enzyme concentration. Linear regression lines fitted to these plots were essentially parallel, and the mean distance between them was used as a measure of relative activity. Membranes from the *pla*$^-$ control strain BL21(DE3, pBS KS$^-$) had no detectable activity.
13. P. M. Stoppelli *et al.*, *Cell* **45**, 675 (1986).
14. O. A. Sodeinde and J. D. Goguen, *Infect. Immun.* **57**, 1517 (1989).
15. Five micrograms of factor B or C3 were incubated alone, with *pla*$^-$ *E. coli* outer membranes (400 ng of total protein), or with *pla*$^+$ outer membranes (400 ng of total protein, 200 ng of Pla). The reaction mixtures were then analyzed by electrophoretic separation on denaturing gels. Factor B was unaffected by any of these treatments, whereas the α chain of C3 had higher mobility after treatment with *pla*$^+$ membranes, indicating removal of a fragment of about 10 kD.
16. D. L. Dunn and R. L. Simmons, *Surgery* **92**, 513 (1982).
17. P. Mignatti, E. Robbins, D. B. Rifkin, *Cell* **47**, 487 (1986).
18. R. Rosqvist, M. Skurnik, H. Wolf-Watz, *Nature* **334**, 522 (1988).
19. L. J. Reed and H. Muench, *Am. J. Hyg.* **27**, 493 (1938).

20. Supported by grant AI22176 from the National Institutes of Health (J.G.). We thank I. Joris, G. Mano, and D. Tipper for discussions, M. Apple for histological preparations, and Yi Bao for general technical assistance.

1 June 1992; accepted 28 July 1992

Activity-Dependent Decrease in NMDA Receptor Responses During Development of the Visual Cortex

Giorgio Carmignoto* and Stefano Vicini

Plasticity of the developing visual system has been regarded as the best model for changes of neuronal connections under the influence of the environment. *N*-methyl-D-aspartate (NMDA) receptors are crucial for experience-dependent synaptic modifications that occur in the developing visual cortex. NMDA-mediated excitatory postsynaptic currents (EPSCs) in layer IV neurons of the visual cortex lasted longer in young rats than in adult rats, and the duration of the EPSCs became progressively shorter, in parallel with the developmental reduction in synaptic plasticity. This decrease in NMDA receptor–mediated EPSC duration is delayed when the animals are reared in the dark, a condition that prolongs developmental plasticity, and is prevented by treatment with tetrodotoxin, a procedure that inhibits neural activity. Application of L-glutamate to outside-out patches excised from layer IV neurons of young, but not of adult, rats activated prolonged bursts of NMDA channel openings. A modification of the NMDA receptor gating properties may therefore account for the age-dependent decline of visual cortical plasticity.

In the visual cortex, activation of the NMDA subtype of glutamate receptor contributes to normal excitatory synaptic transmission (*1*) and is required for the experience-dependent modifications of synaptic connections that occur during a restricted period of early postnatal development in kittens (*2*). After the animal reaches adulthood, the cortical synaptic organization can no longer be modified by visual experience (*2*). To test whether this reduction in plasticity is associated with a modification of NMDA receptor responses, we studied functional properties of the NMDA receptor in visual cortical neurons of the rat during development, from the time before eye opening to adulthood. We used whole cell and excised patch current recordings in brain slices (*3–5*) from 163 neurons located in layer IV out of a total of 198 visual cortical neurons (*6*).

We studied NMDA responses by analyzing the EPSC evoked by stimulation of the borders between the white matter and layer VI (*7*). In all neurons with voltages clamped at −70 mV holding potential, the EPSC was composed of a fast-decaying component (*8*), which was abolished by the non-NMDA receptor antagonist 2,3-dihydroxy-6-nitro-7-sulfamoyl-benzo(*F*)quinoxaline (NBQX) (10 μM), and a slower tail. This latter component was mediated by NMDA receptors because it was abolished by the selective NMDA antagonist 3-[(±)-2-2-carboxypiperazin-4-yl]-propyl-1-phosphonic

FIDIA Georgetown Institute for the Neurosciences, Georgetown University School of Medicine, 3900 Reservoir Road, NW, Washington, DC 20007.

*To whom correspondence should be addressed.

acid (CPP) (10 μM) (n = 10). In all experiments, NMDA receptor–mediated EPSCs (NMDA-EPSCs) were studied after prolonged washing with a nominally Mg^{2+}-free solution in the presence of 10 μM NBQX and 1 μM glycine (9).

During development, in 13 spiny stellate neurons and 42 pyramidal layer IV neurons from rats of various ages, amplitudes and rise times of NMDA-EPSCs did not significantly change [amplitude, 75 ± 36 pA (mean ± SD); range, 21 to 161 pA] (rise time, 6.9 ± 3.3 ms; range, 4.1 to 10.9 ms) (−50 mV holding potential). In contrast, the duration of NMDA-EPSCs decreased. Before eye opening, at 9 to 14 days, NMDA-EPSC decays (7) were well described by either a single (range, 180 to 390 ms; n = 10) (Fig. 1A) or double exponential function with a fast and slow component (τ_f, range, 21 to 63 ms; τ_s, range, 177 to 321 ms; n = 8). However, the relative contribution of the slow component to the EPSC was dominant (average, 92 ± 12% of the total current; n = 18). To investigate whether the slow decay of evoked NMDA-EPSCs was due to temporally uncorrelated polysynaptic activity, we also recorded miniature NMDA-EPSCs (10). The miniature NMDA-EPSCs were mediated by NMDA receptors because they were recorded in the presence of 10 μM NBQX and disappeared after perfusion with 10 μM CPP. The average time constants for the decay of miniature NMDA-EPSCs were similar to those of evoked NMDA-EPSCs (Fig. 1A).

Faster NMDA-EPSCs were observed in neurons from older rats. The average decay of NMDA-EPSCs from layer IV neurons at day 35 was always best described by a double exponential function (τ_f, range, 35 to 66 ms; τ_s, range, 171 to 301 ms; n = 8) (Fig. 1B). The slow component, however, was never greater than 35% of the total current. Miniature NMDA-EPSCs recorded from six neurons were also very fast (Fig. 1B); their duration was well correlated with that of evoked synaptic currents.

The NMDA-EPSC was voltage-dependent and reversed at a holding potential of +5 ± 6 mV; its duration at −50 mV holding potential (Fig. 1C) and at +50 mV holding potential (Fig. 1C, inset) (11) progressively decreased with the age of the rat. The relative contribution to the NMDA-EPSC of the slow component decreased from 90% at day 12 to less than 20% in two 4-month-old rats. Because the time constants of the fast and slow components remained unchanged during the same period (Fig. 1D), the progressive decrease of the slow component contribution of the NMDA-EPSC accounts for the faster currents in adult rats. A developmental increase in the sensitivity of NMDA-EPSCs to the residual Mg^{2+} (12) cannot by itself account for the reduction in duration because it was also observed at a +50 mV holding potential (Fig. 1C, inset). However, we did not directly compare the Mg^{2+} (12) and glycine (9) sensitivity of the NMDA receptor in young and in fully developed rats. The kinetic changes of the NMDA-EPSC were similar in pyramidal and stellate cells of layer IV (13). We also observed shortening in the duration of NMDA-EPSCs during development in neurons located in layers other than layer IV (n = 32).

To examine the mechanism underlying the developmental decrease of the NMDA-EPSC duration (14), we investigated NMDA channel currents elicited by L-glutamate in outside-out patches (15). We hypothesized that a modification of the intrinsic functional properties of postsynaptic receptors results in short-lasting synaptic

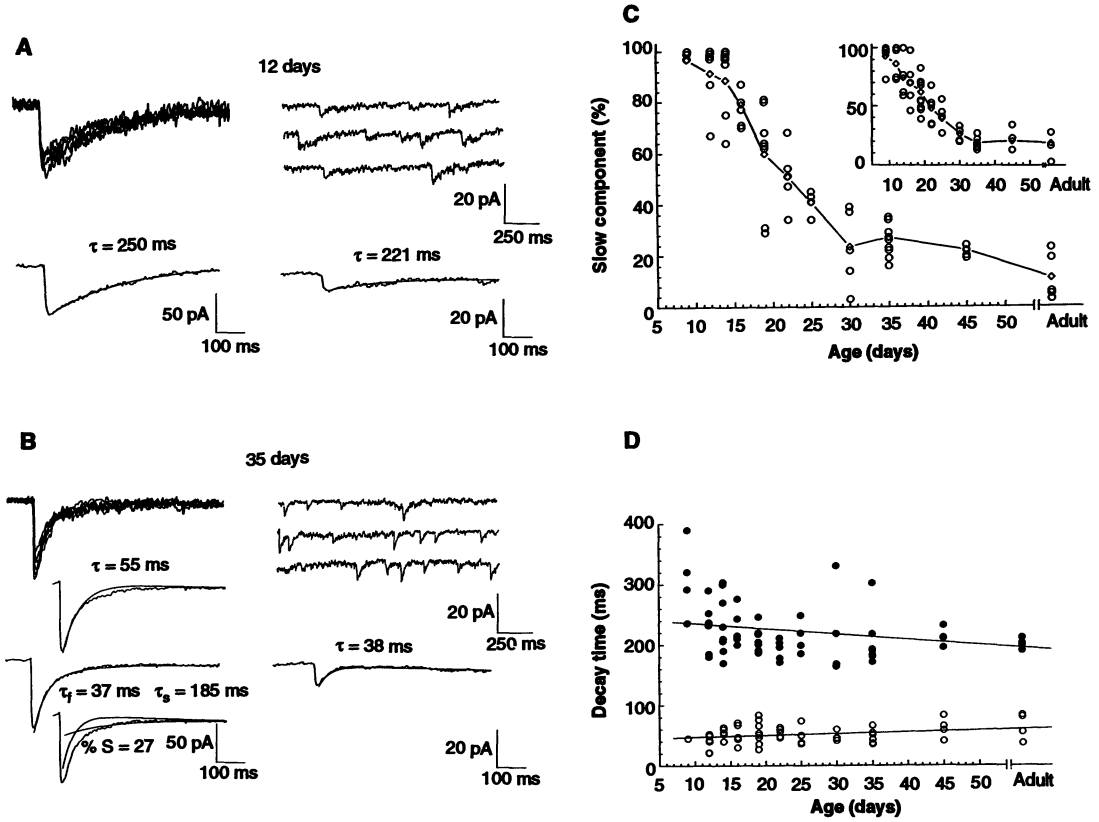

Fig. 1. Kinetic changes of NMDA-EPSCs from layer IV neurons. (**A** and **B**) Five superimposed EPSCs (top left) followed by the average of 20 consecutive events (bottom right) obtained from a stellate cell of (A) a 12- and (B) a 35-day-old rat. In (A), the single exponential curve of the decay is superimposed on the average current (bottom right). In (B), the poor single exponential fitting is followed by the superimposed double exponential curve with fast and slow components also shown (bottom right). Spontaneous NMDA-EPSCs at −50 mV holding potential are also shown in the top left panels of (A) and (B). Bottom traces (left) are the average of 30 events with the superimposed single exponential curve. The average decay of miniature NMDA-EPSCs from six neurons of 12-day-old rats is 221 ± 84 ms (n = 145) and from six neurons of 35-day-old rats is 45.9 ± 17 ms (n = 182). The amplitudes (range, 5 to 45 pA) and rise times (range, 4.8 to 10.5 ms) did not significantly differ with age; f, fast component; s, slow component. (**C**) Developmental decrease of the slow component contribution to NMDA-EPSC at −50 and +50 mV (inset) holding potentials. Lines connect the averages (diamonds) of the experimental points (circles). One-way analysis of variance (ANOVA) with subsequent comparison by the Duncan multiple range test showed that the slow component contributions to EPSCs from rats at different ages were statistically different ($P < 0.05$) between 12- to 14-day-old rats and rats older than 16 days. The label "adult" refers to two 4-month-old rats. (**D**) Time constants of the fast and slow exponential decays at −50 mV holding potential. Filled circles represent the τ_s and empty circles the τ_f. The only statistically significant difference was for the τ_s of 9-day-old rats ($P < 0.05$, ANOVA followed by the Duncan test).

currents, although presynaptic differences such as the type of neurotransmitter (16), its reuptake, and the kinetics of vesicular release could also contribute.

A brief (4 ms) application of L-glutamate (1 mM) to outside-out patches from layer IV neurons (n = 9) (holding potential, −50 mV) of rats before eye opening (12 to 14 days old) induced the synchronous activation of many NMDA channels, followed by the occurrence of multiple clusters of openings (16) well after the termination of the L-glutamate pulse (Fig. 2A). The average current had a double exponential decay (τ_f, range, 28 to 51 ms; τ_s, range, 156 to 460 ms) (Fig. 2A, left). The slow component was largely dominant (Fig. 2B), comprising on average 88 ± 17% of the total current. In contrast, in patches from neurons of 30- to 35-day-old rats (n = 15; holding potential, −50 mV), the duration of channel opening clusters was dramatically shorter (Fig. 2A, right). The average decay was also best fitted with a double exponential (τ_f, range, 10 to 78 ms; τ_s, range, 128 to 374 ms; slow component, 34 ± 22% of the total current) (Fig. 2C). The similarity of the NMDA current decays between excised patch and whole cell recordings (Fig. 2C) suggests that the duration of NMDA channel opening clusters accounts for the decay of the synaptic currents (16). This finding also implies that a change in the gating properties of NMDA receptors may account for the developmental decrease of the NMDA-EPSC duration. Recently, a developmental decrease in the duration of NMDA-EPSCs recorded from neurons in the superior colliculus has also been reported (17).

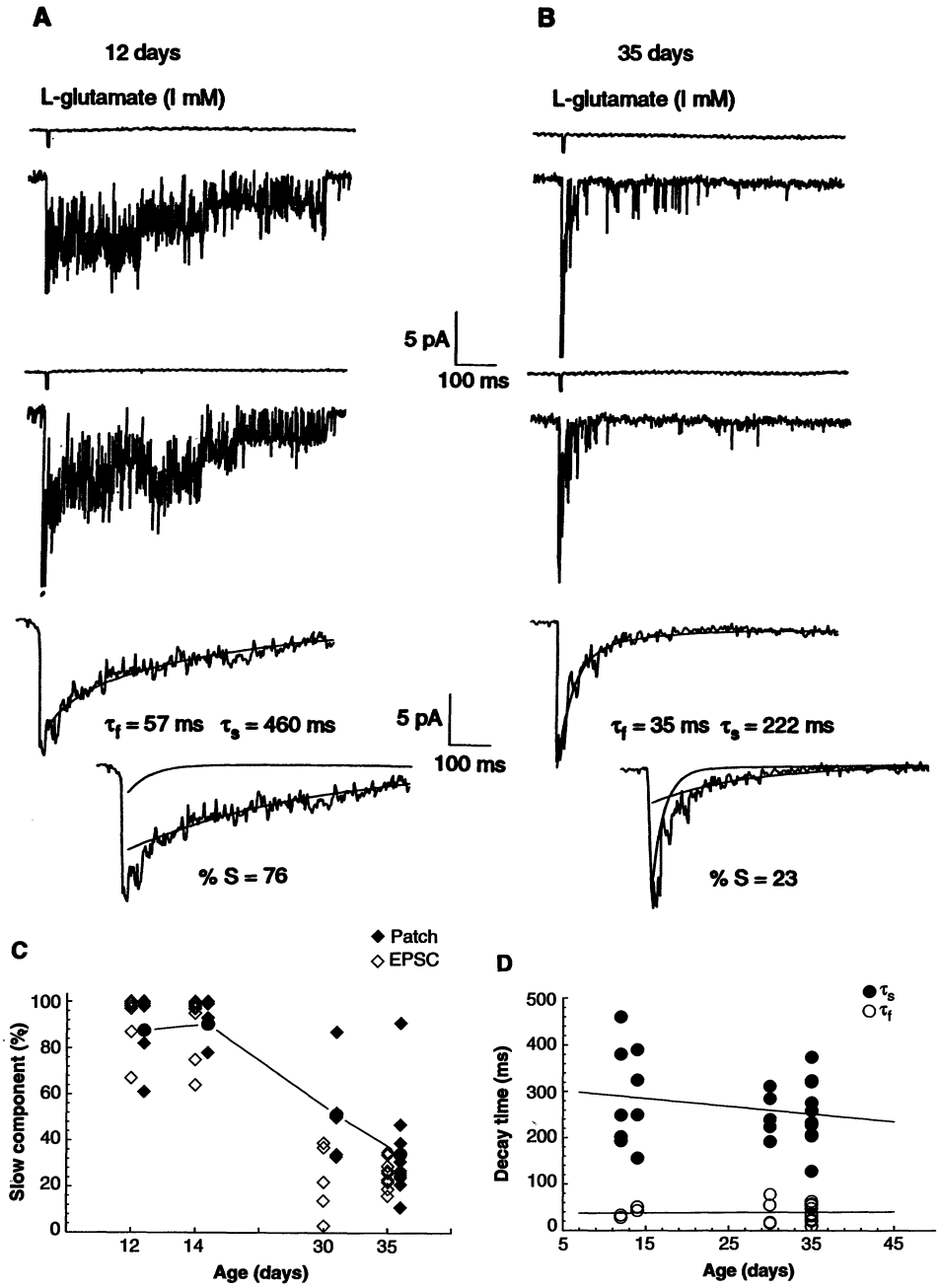

Fig. 2. Kinetic changes of NMDA channel currents activated by 4-ms application of L-glutamate in (**A**) a 12-day-old rat and (**B**) a 35-day-old rat. Two consecutive responses (top) and the average current (bottom) of 20 consecutive L-glutamate applications shown with a superimposed double exponential curve with fast and slow components are shown independently. The open-tip current used to measure the duration of the drug application pulse is shown above each of the two channel current traces. The amplitude calibration bar does not apply to these traces. The single channel current amplitude did not differ at the two ages considered [−50 mV holding potential, 2.7 ± 0.51 pA at 12 to 14 days after birth (n = 9) and 2.7 ± 0.45 pA at 30 to 35 days after birth (n = 15)]. (**C**) Developmental decrease of the slow kinetic component to NMDA-EPSC (same data as in Fig. 1) and average NMDA channel currents. Differences between young (12 to 14 days) and old (30 to 35 days) rats were statistically significant (P < 0.05, ANOVA followed by the Duncan test). (**D**) Time constants of the fast and slow exponential decays of average NMDA channel currents.

Changes in NMDA receptor gating during development of the visual system might correlate with a general decline of visual cortical plasticity. Therefore, we examined whether rearing rats in complete darkness would delay the age-dependent change of NMDA receptors. Three rat litters were reared in the dark from birth until the day of recording. In a total of 49 neurons in layer IV of 12 rats, dark-rearing delayed the developmental shortening of NMDA-EPSC duration; however, amplitudes and rise times of these currents were not affected. The average NMDA-EPSC decay in dark-reared rats (19 to 45 days) was best described by two exponentials (τ_f, range, 23 to 82 ms; τ_s, range, 162 to 259 ms; n = 49) (Fig. 3). The slow component of NMDA-EPSCs was significantly larger in rats reared in the dark than in rats reared in the light (Fig. 3). This result is consistent with our hypothesis that the developmental decrease of the NMDA-EPSC duration plays a crucial role in the synaptic plasticity of the developing visual cortex, and the decrease may represent a cellular mechanism for the reduction of NMDA receptor function reported to occur in vivo during the normal development of the kitten visual cortex (18). However, more direct evidence is needed to extend these results to a "critical period" of visual cortical development in the rat (19).

Rearing an animal in the dark results in suppressed visual stimuli–induced neuronal activity but not intrinsic cortical activity. By administering daily intracortical injections of tetrodotoxin (TTX) (20), we dras-

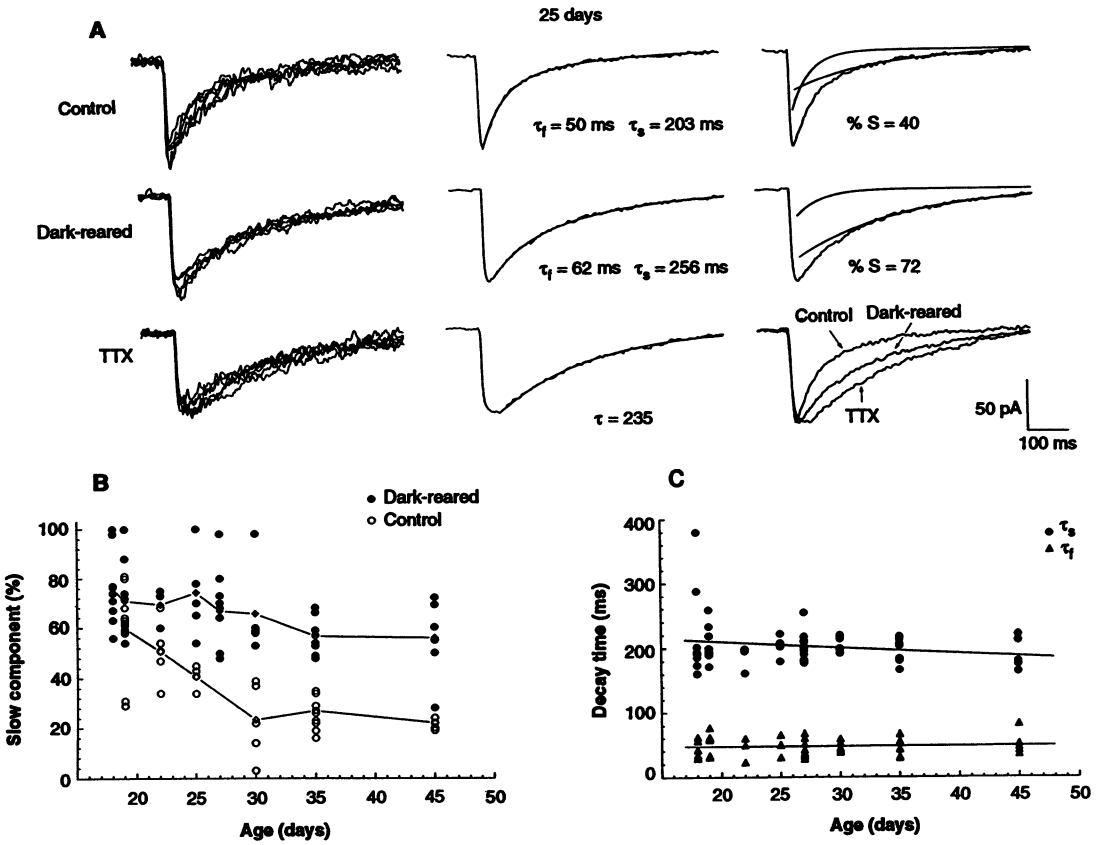

Fig. 3. Effects of dark-rearing and TTX intracortical treatment on the developmental change of NMDA-EPSCs. (**A**) Five overlapping EPSCs from 25-day-old rats reared in the three different conditions (left) followed by the ensemble average of 20 consecutive events with superimposed double exponential curve (middle) and double exponential fittings (right). (**B**) Developmental decrease of the slow component of NMDA-EPSC in control and dark-reared rats. Statistical analysis of control versus dark-reared animals at different ages showed significant differences in rats older than postnatal day 22 ($P < 0.05$, two-way ANOVA followed by the Duncan test). (**C**) The time constants of the fast and slow exponential decays of the EPSCs in dark-reared rats.

tically reduced neuronal activity in the visual cortex. The NMDA-EPSC from 20 layer IV neurons of two TTX-treated rats (slow component, 90 ± 12% of the total current; τ_f, range, 31 to 62 ms; τ_s, range, 186 to 394 ms) had a larger slow component than that from neurons of age-matched dark-reared rats (Fig. 3A). This result further strengthens our hypothesis that the developmental change of NMDA-EPSCs, which is prevented by TTX (Fig. 3A, bottom traces), is under the tight control of neuronal activity.

The activity-dependent modification of NMDA receptor gating properties during development might be related to a subunit substitution in the NMDA receptor composition, similar to the changes that occur in acetylcholine receptors at the developing neuromuscular junction (*21*). Molecular cloning has demonstrated that NMDA receptors are hetero-oligomeric integral membrane proteins (*22*, *23*). Moreover, in recombinant NMDA receptors, L-glutamate activates channel currents with a different relaxation decay, depending on the subunit composition of the receptor (*23*), with time constants that correspond well with our measurements.

A long-lasting NMDA-EPSC, mediating Ca^{2+} influx and the subsequent intracellular events (*24*), serves to strengthen synaptic connections. The progressive shortening of NMDA-EPSC duration during development, which is dependent on sensory experience, is related to the progressive reduction of synaptic plasticity operative in visual cortical development. The decrease of NMDA-EPSC duration might constitute a general mechanism that controls the conversion from a synapse capable of manifesting plasticity to a stable, less plastic synapse, perhaps by modification of the expression of functionally distinct NMDA receptor subtypes.

REFERENCES AND NOTES

1. K. D. Miller, B. Chapman, M. P. Stryker, *Proc. Natl. Acad. Sci. U.S.A.* **86**, 5183 (1989).
2. C. R. Olson and R. D. Freeman, *Exp. Brain Res.* **39**, 17 (1980); N. Daw, K. Fox, H. Sato, D. Czepita, *J. Neurophysiol.* **67**, 197 (1992); J. P. Rauschecker, *Physiol. Rev.* **71**, 587 (1991).
3. O. P. Hamill, A. Marty, E. Neher, B. Sakmann, F. J. Sigworth, *Pfluegers Arch.* **391**, 85 (1981).
4. F. A. Edwards, A. Konnerth, B. Sakmann, T. Takahashi, *ibid.* **414**, 600 (1989).
5. P. Stern, F. A. Edwards, B. Sakmann, *J. Physiol. (London)* **449**, 247 (1992).
6. Coronal slices of occipital neocortex (200 to 300 μm) were prepared from Sprague-Dawley rats (*4*). In previous experiments, we used the retrograde transport of a fluorescent tracer after injection into the lateral geniculate nucleus (fast blue, 1 to 3 μl of 5% solution in water) (Sigma) to identify the anatomical markers of the coronal sections, including the visual cortex in developing rats. Slices were submerged in 500 μl of Ringer solution and continuously perfused (5 ml/min). Ringer solution contained 120 mM NaCl, 3.1 mM KCl, 1.25 mM NaH_2PO_4, 25 mM $NaHCO_3$, 5 mM dextrose, 1 mM $MgCl_2$, 2 mM $CaCl_2$, bicuculline methiodide (BMI, 20 μM) (Sigma), and glycine (10 μM) (Sigma); the solution was maintained at pH 7.4 with 5% CO_2–95% O_2. Excitatory amino acid receptor antagonists [J. C. Watkins, P. Krogsgaard-Larsen, T. Honoré, *Trends Pharmacol. Sci.* 11, 25 (1990)] CPP (Tocris, Buckhurst Hill, U.K.) and NBQX were dissolved in water and diluted in Ringer solution. Patch pipettes (*3*) (resistance, 5 to 8 megohms) were filled with 110 mM potassium gluconate, 35 mM cesium gluconate, 1 mM $MgCl_2$, 5 mM EGTA, 2 mM sodium adenosine triphosphate, 0.2 mM guanosine triphosphate, and 11 mM Hepes; the solution was maintained at pH 7.2 with CsOH. To stain recorded cells, we diluted Lucifer yellow (4 mg/ml) (Sigma) in the pipette solution. Whole cell recordings were performed in current- and voltage-clamp with a patch-clamp amplifier (EPC 7, List Electronics, Darmstad, Germany). Series resistance (10 to 20 megohms) was compensated and checked for constancy throughout the experiments. We measured the action potential (AP) firing pattern by injecting depolarizing current pulses before AP lengthening induced by the cesium gluconate, and it was classified according to the system of A. McCormick, B. W. Connors, J. W. Lighthall, and D. Prince [*J. Neurophysiol.* **54**, 782 (1985)]. All aspiny stellate cells were fast-spiking (*5*), whereas pyramidal and spiny stellate cells were regular-spiking (*5*) as well as intrinsically bursting (*5*). With Nomarski optics (UEM, Zeiss, Germany), layer IV was clearly distinguishable as a high-density band of small cells. With the use of Lucifer yellow staining, we classified recorded neurons in distinct morphological types (pyramidal and spiny or aspiny stellate) and identified (from photomicrographs taken for each cell) their layer location. In this study, we used rats rather than kittens because they are more amenable to patch-clamp recordings in brain slices. We focused our study mainly on layer IV neurons because they are the main target of geniculo-cortical afferents and because previous work described developmental changes in vivo in kittens as occurring mainly in layer IV neurons [K. Fox *et al.*, *J. Neurosci.* **9**, 2443 (1991)].

7. EPSCs were evoked by stimuli consisting of 50-μs pulses (50 to 200 μA at 0.2 Hz) applied through a bipolar tungsten electrode (5-μm tip, Roboz, Maryland) to the layer VI border of the white matter. EPSCs likely derive from excitatory afferents containing geniculo-cortical projections, which represent the main component of the excitatory input to layer IV neurons from subcortical structures, as well as from intrinsic cortical connections [L. C. Katz and E. M. Callaway, *Annu. Rev. Neurosci.* **15**, 31 (1992)]. Current and voltage signals were filtered at 0.5 to 2 kHz (eight-pole low-pass Bessel LP902, Frequency Devices, Haverhill, MA), and events were recorded on magnetic tape (VR 10-A, Instrutech Corporation, Elmont, NY). Off-line analysis was performed with an LSI 11/73 computer (Indec System, Sunny Vale, CA) after digitization (1 to 5 kHz). A single or double exponential equation of the form

$$I(t) = I_f\exp(-t/\tau_f) + I_s\exp(-t/\tau_s)$$

where I is the current amplitude, t is time, I_f and I_s are the peak amplitudes, and τ_f and τ_s are their respective time constants of fast and slow components, was used to describe the EPSC and channel current average decays with an entirely automated least-squares procedure [see S. Vicini and S. M. Schuetze, *J. Neurosci.* **5**, 2212 (1985) for further details]. EPSC amplitudes were measured, and the noise of the baseline and noise around the peak were taken into account. Rise times represent the time elapsed from 20 to 80% of the peak amplitude of the response.
8. Non-NMDA receptor–mediated EPSCs failed to change from 10 to 45 days after the birth of the rats (amplitude, range, 21 to 260 pA; rise time, range, 0.3 to 1.2 ms), and the mean decay time constant was 10.5 ± 4.5 ms from days 12 to 16 and 11.9 ± 3.7 ms from days 27 to 45. Non–NMDA-EPSCs from aspiny stellate neurons (n = 11) were faster (decay, range, 0.9 to 3.9 ms), as reported (*5*).
9. J. W. Johnson and P. Ascher, *Nature* **325**, 529 (1987).
10. Sucrose (300 mM) (Sigma) was pressure-applied (2 to 4 pounds per square inch for 5 s) locally through a large-diameter (5 to 10 μm) patch-pipette in the presence of TTX (1 μM).
11. Average NMDA-EPSC values were obtained from at least 20 consecutive events recorded initially at +50 mV and then at −50 mV holding potential. The decay time constants were slower at positive than at negative holding potentials; we failed, however, to observe the voltage-related twofold to threefold difference reported in hippocampal neurons [A. Konnerth, B. U. Keller, K. Ballanyi, Y. Yaari, *Exp. Brain Res.* **81**, 209 (1990)].
12. N. W. Kleckner and R. Dingledine, *Mol. Brain Res.* **11**, 151 (1991).
13. G. Carmignoto and S. Vicini, unpublished results.
14. Differences in the kinetics of NMDA-mediated EPSCs in spiny stellate and pyramidal visual cortical neurons were probably not the result of poor spatial voltage control for several reasons. (i) Non–NMDA-EPSC kinetics were similar in young and adult rats (*8*). (ii) In 11 stellate aspiny cells, the NMDA-EPSC decay is also described by the sum of two exponentials with similar time constants (τ_f, 35 to 73 ms; τ_s, 130 to 291 ms). As suggested by Stern *et al.* (*5*), excitatory synapses on these cells are located on or close to the soma, thereby under adequate space-clamp control. (iii) The time constants of currents from patches and from synapses are similar (see Fig. 2A).
15. Average NMDA currents in excised patches were obtained from at least 20 consecutive applications of L-glutamate with a fast application system that changed solution by switching the flow from the two sides of a theta tubing with a tapered tip of 200 μm. The theta tubing contained Mg^{2+}-free Ringer solution with NBQX (10 μM) and glycine (10 μM) in one of the two compartments, and in the other it contained the same solution with the addition of L-glutamate (1 μM) diluted 50:1 with water (*16*); this dilution permitted measurement of the duration of the drug application pulse by recording the open tip current at the end of each experiment (*16*).
16. R. A. J. Lester and C. E. Jahr, *J. Neurosci.* **12**, 635 (1992).
17. S. Hestrin, *Nature* **357**, 686 (1992).
18. K. Fox, N. Daw, H. Sato, D. Czepita, *ibid.* **350**, 342 (1991).
19. J. G. Parnavelas and A. Globus, *Exp. Neurol.* **51**, 637 (1976); J. Cronly-Dillon and G. W. Perry, *J. Physiol.* (*London*) **293**, 469 (1979); C. A. Stafford, *Ophthalmic Physiol. Opt.* **4**, 95 (1984); L. Domenici, N. Berardi, G. Carmignoto, G. Vantini, L. Maffei, *Proc. Natl. Acad. Sci. U.S.A.* **88**, 8811 (1991); N. Berardi *et al.*, *J. Physiol.* (*London*) **434**, 14 (1991).
20. We injected 1 to 2 μl of TTX (500 μM in citrate buffer) (Sigma) intracortically every day, beginning at 14 days after birth for 10 days. Injections were made through a small hole in the skull (at stereotaxic coordinates 1 mm lateral and 3 mm posterior to bregma) with a glass pipette (50-μm tip). The weight of treated rats at 25 days was in the same range as that of the controls before they were killed. We performed an independent check of the effects of TTX 6 hours after TTX injection by monitoring visual evoked potential in response to alternating gratings of various spatial frequencies and contrast.
21. M. Mishina *et al.*, *Nature* **321**, 406 (1986); W. Witzemann, B. Barg, Y. Nishikawa, B. Sakmann, S. Numa, *FEBS Lett.* **223**, 104 (1987).
22. K. Moriyoshi *et al.*, *Nature* **354**, 31 (1991).
23. H. Monyer *et al.*, *Science* **256**, 1217 (1992).
24. M. L. Mayer and R. J. Miller, *Trends Pharmacol. Sci.* **11**, 254 (1990).

25. We thank the late S. M. Schuetze for the curve-fitting computer program; E. Costa, L. Maffei, and C. T. Livsey for helpful comments; and L. Nordholm (Novo Nordisk, Denmark) for providing NBQX. Supported by the National Institute of Neurological and Communicative Disorders and Stroke program project grant PO1 NS 28130-01.

15 June 1992; accepted 14 September 1992